Volume Title
ASP Conference Series, Vol. **Volume Number**
Author
© **Copyright Year** Astronomical Society of the Pacific

Prediction of Observing Conditions for DES Exposure Scheduling

Eric H. Neilsen, Jr.

Fermi National Accelerator Laboratory,
P.O. Box 500, Batavia, IL 60510, USA.

Abstract. Delivered sky brightness and atmospheric seeing are two important factors in the optimal scheduling of observations in large observing programs, but are less well studied than spherical astronomy. In the Dark Energy Survey (DES), planning software needs to optimize over the requirements of each of its science programs. For example, observing cadence is the primary factor in supernova detection, whereas seeing is the most important factor in weak lensing measurements. Delivered sky brightness is an important factor in filter and field selection for all programs. I describe models for the short timescale (5 minute) evolution of seeing and delivered sky brightness, and parametrize and test these models using data from CTIO and Apache Point Observatory.

1. DES Exposure Scheduling

The Dark Energy Survey (DES) will study dark energy using four complementary techniques: type Ia supernovae (SN), baryon acoustic oscillations (BAO), galaxy clusters (GC), and weak gravitational lensing (WL). The DES observing program consists of two surveys: a narrow survey used to collect SN light-curves, and a wide-field survey used by the other techniques. The two surveys have different observing constraints: the fields in the narrow survey must be observed according to a regular observing cadence, while the weak lensing science is more sensitive to seeing. All programs need to avoid fields with high background surface brightness. Optimal execution of the program therefore depends on scheduling exposures based on current conditions.

SISPI, the DES data acquisition and control system, will execute DES science program by following an observing queue. The queue is a list of exposures that can be viewed and edited both by the observatory staff and the Observation Tactics program, ObsTac. During observing, ObsTac monitors the length of the observing queue and, when the length fall below a configurable duration, adds new observations to the queue according to the survey footprint and global strategy, the estimated quality of completed exposures, the current contents of the queue, the positions of needed fields on the sky, and estimates of the weather conditions (seeing, cloudiness, and sky brightness) at the extrapolated time of observation.

ObsTac therefore relies on models to predict the seeing and sky brightness for candidate observations. Furthermore, the simulations used to evaluate and optimize the selection algorithms used by ObsTac require realistic simulation of seeing and sky brightness to be effective.

2. A Model for Sky Brightness

The luminosity of the night sky arises from several sources: airglow, scattered moonlight, light pollution, unresolved astronomical sources, zodiacal light, gegenschein, and polar aurorae. This model only includes explicit models of airglow (using the model van Rhijn (1921)) of and scattered moonlight (using a combination of Rayleigh scattering and Mie scattering as approximated by the formula proposed by Cornette & Shanks (1992)); it accounts for other sources with a constant background (fit to the dark sky with the airglow) and a simple function of time of night, time of year, azimuth, and airmass fit to the residuals after the subtraction of other sources.

The model parameters such as the airglow height were fit to data from the Sloan Digital Sky Survey (SDSS) photometric telescope (PT), used to calibrate and monitor sky conditions for the SDSS. The PT collected more than 20,000 sequences of 5 exposures (one in each of the 5 SDSS filters) between 1999 and 2008, including many with bright moonlight (Tucker et al. 2006). First, I fit the airglow height and luminosity and constant background to exposures without moonlight. Then, I fit the Rayleigh scattering of moonlight to exposures for which the angle between the moon and the exposure's pointing was between 40 and 100 degrees, where such scattering is expected to dominate Mie. I then fit the Mie scattering parameters to the remaining flux. Finally, I fit the residuals to a simple function of airmass, azimuth, time of day, and time of year to accommodate other sources.

3. Autoregressive Time Series Analysis

Even after fits to obvious astronomical and positional parameters have been subtracted, significant residuals remain. These residuals are strongly correlated in time, suggesting that a good estimate of the offset from the model in the near future is the offset from the model in the recent past. Such an estimate corresponds to a model in which the offset from the model follows a random walk. While such a model is likely to be adequate for prognostication, it cannot represent the underlying process, or be used to generate realistic data for simulations, because in such a model the offset from the model will grow linearly with time. An autoregressive model (Cryer & Kung-Sik 2010), in which the offset at time t is the weighted mean of the global mean offset and some number of previous time steps, overcomes this problem. For this model, the mean offset is zero and a linear combination of the two previous time steps accounts for most temporal correlation. In the r filter, for example, the best fit AR(2) model for the offsets is:

$$\Delta D_t = 0.70\Delta D_{t-1} + 0.13\Delta D_{t-2} + e_t$$

where e_t follows a normal distribution with variance 0.013, resulting in an uncertainty of $0.11\mathrm{mag/asec}^2$ when ΔD_t is estimated as $0.70\Delta D_{t-1} + 0.13\Delta D_{t-2}$. Over time, the uncertainty relative to the global model tends to $0.17\mathrm{mag/asec}^2$ rather than increasing with time indefinitely. Figure 1 shows the overall effect of applying the AR(2) model.

4. Seeing Variability

An autoregressive time series analysis is also useful for modeling seeing variability. Els et al. (2009) studied seeing data for CTIO, and found significant variation on yearly

Figure 1. A comparison of the static and AR(2) modeled sky brightness on SDSS PT r band data, resampled into 1 hour intervals.

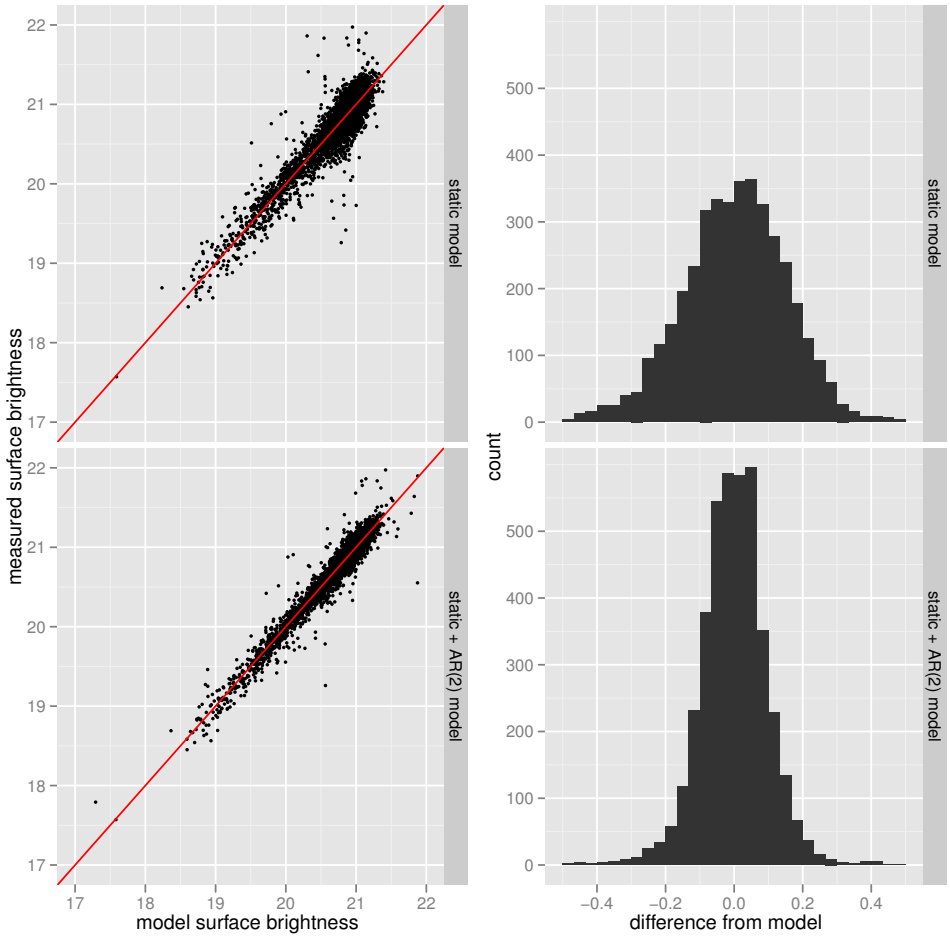

time scales. For shorter time scales, an autoregressive analysis on a series of seeing values derived from mean DIMM measurements from the CTIO database, resampled into 5 minute intervals, results in:

$$s_t = 0.48 s_{t-1\mathrm{day}} + 0.13 s_{t-10\mathrm{min}} + 0.80 s_{t-5\mathrm{min}} + e_t;\ s_t = f(\mathrm{FWHM}_t)$$

where f is a reversible monotonic function that transforms the skew-log-normal seeing distribution to an approximate normal distribution, and e_t is normally distributed with a standard deviation of 0.38. The value $s = 0.0$ corresponds to a PSF with FWHM = $0.76''$ and $s = 0.38$ corresponds to FWHM = $0.87''$, indicating variations of order $0.1''$ are introduced in each 5 minute time interval. Indeed, the differences between predictions made with this model ($s_{t,\mathrm{pred}} = 0.48 s_{t-1\mathrm{day}} + 0.13 s_{t-10\mathrm{min}} + 0.80 s_{t-5\mathrm{min}}$) and measured values have a standard deviation of $0.13''$. The median absolute deviation is only $0.06''$ and distribution has a high kurtosis of 17.7; small and large deviations are significantly more common than would be predicted by a normal distribution. Figure 2 shows a comparison of the measured and predicted values.

Figure 2. Comparisons of the AR model for seeing variation and DIMM values

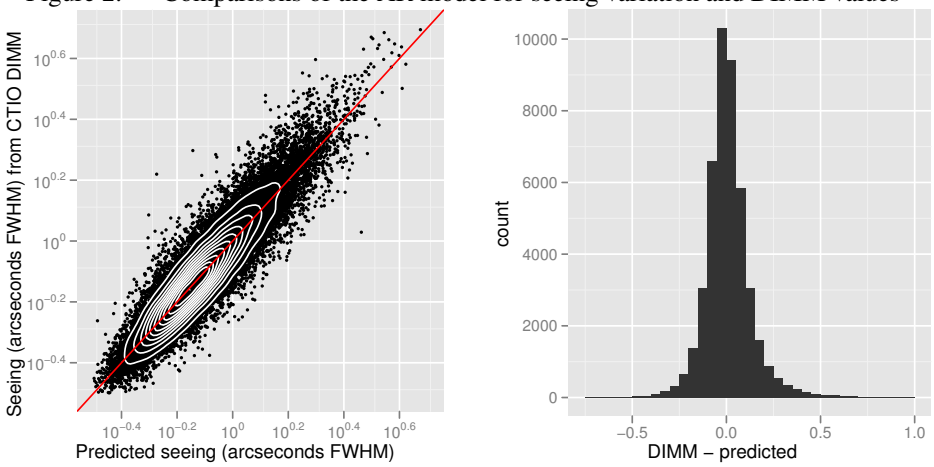

References

Cornette, W. M., & Shanks, J. G. 1992, Appl. Opt., 31, 3152
Cryer, J., & Kung-Sik, C. 2010, Time Series Analysis With Applications in R (New York: Springer), 2nd ed.
Els, S. G., Schöck, M., et al. 2009, PASP, 121, 922
Tucker, D. L., Kent, S., et al. 2006, Astronomische Nachrichten, 327, 821
van Rhijn, P. J. 1921, Publications of the Kapteyn Astronomical Laboratory Groningen, 31, 1

Acknowledgments. Funding for the DES Projects has been provided by the U.S. Department of Energy, the U.S. National Science Foundation, the Ministry of Science and Education of Spain, the Science and Technology Facilities Council of the United Kingdom, the National Center for Supercomputing Applications at the University of Illinois at Urbana-Champaign, the Kavli Institute for Cosmological Physics at the University of Chicago, Financiadora de Estudos e Projetos, Fundacao Carlos Chagas Filho de Amparo a Pesquisa do Estado do Rio de Janeiro , Conselho Nacional de Desenvolvimento Cientifico e Tecnologico and the Ministerio da Ciencia e Tecnologia, and the Collaborating Institutions in the Dark Energy Survey.

The Collaborating Institutions are Argonne National Laboratories, the University of Cambridge, Centro de Investigaciones Energeticas, Medioambientales y Tecnologicas-Madrid, the University of Chicago, University College London, DES-Brazil, Fermilab, the University of Edinburgh, the University of Illinois at Urbana-Champaign, the Institut de Ciencies de l'Espai (IEEC/CSIC), the Institut de Fisica d'Altes Energies, the Lawrence Berkeley National Laboratory, the University of Michigan, the National Optical Astronomy Observatory, the Ohio State University, the University of Pennsylvania, the University of Portsmouth, and the University of Sussex.

Fermilab is operated by Fermi Research Alliance, LLC under Contract No. DE-AC02-07CH11359 with the United States Department of Energy.